

Ultrasensitive magnetometry using quantum-based sensor technology

Lutz Trahms¹

Sensors are vitally important tools for various technologies, such as, e.g., navigation, geo-prospecting, or the characterization of biological or chemical materials. The exploitation of quantum phenomena offers the chance to develop novel powerful sensors to be applied in ultra-high-precision spectroscopy, positioning systems, clocks, gravitational, electrical and magnetic field measurements, and optical resolution beyond the wavelength limit. Quantum-based sensing technologies are increasingly important in fundamental research from the sub-nano to the galactic scale, as well as for the determination of the fundamental constants. But also in applied science, quantum-based sensing has become a powerful research tool, notably in biomedical science and diagnostics.

One of the most advanced applications of quantum sensing is magnetometry. Currently, two approaches of quantum based magnetometry are in a mature state of development, enabling sensitive measurements of magnetic fields at various length and frequency scales:

- Superconducting quantum interference devices (SQUIDs)
- Atomic vapor cells or optically pumped magnetometers (OPMs)

However, the benefit of their outstanding resolution is compromised by the strong contaminations that are inevitably present in any urban laboratory environment. Therefore, a prerequisite for magnetic metrology in the ultra-low field range is the suppression of external perturbations. In PTB we utilize the ultimate shielding performance of the BMSR-2 (Berlin Magnetically Shielded Room 2), where external magnetic perturbations are reduced by many orders of magnitude, and the residual static magnetic field is as low as a few hundred picotesla.

SQUIDs

Only two years after Brian Josephson had postulated the flow of a tunneling current between two superconductors across an insulating barrier, the SQUID was invented [1]. The SQUID represents a closed superconducting loop containing one or two Josephson junctions which encompasses a discrete number of magnetic flux quanta. A change of the external magnetic field results in a voltage across the SQUID that can be taken as a measure of the magnetic field change. A general limitation of SQUIDs is their in practicability to measure the absolute value of the magnetic field.

Since their invention more than fifty years ago, superconducting quantum interference devices are the most sensitive magnetic sensors covering a wide frequency range up to the Megahertz range. During this time, the sensitivity of SQUIDs has increased by several orders of magnitude. PTB was one of the driving forces in this development [2]. Up to now, the SQUID system with the highest sensitivity is PTB's wideband magnetometer with noise level down to 150 attotesla/ $\sqrt{\text{Hz}}$ [3]. Due to this unsurpassed performance, SQUID are considered the metrological reference for ultra-low magnetic fields.

On the other hand, the practical operation of SQUIDs is often hampered by their inflexible handling. To maintain their superconducting state, so-called low temperature (LTc-) SQUIDs are typically mounted in a bath of liquid helium which makes their application cumbersome and difficult, particularly for biomagnetic measurements, i.e. the measurement of magnetic fields generated by ionic currents in the human body. A consequence of their low operation temperature of a few K is that LTc-SQUIDs usually must be kept at a distance of a few centimeters from the investigated objects at room temperature. This problem is mitigated when so-called high temperature (HTc-) SQUIDs

¹ Dr. Lutz Trahms has been the head of department 8.2 "Biosignals" until his retirement in 2019.

Figure 6.1: PTB has been leading in SQUID development during the last 30 years:

Left: “Cart-wheel”-type SQUID magnetometers that achieve a magnetic field noise levels as low as $2\text{--}3\text{ fT}/\sqrt{\text{Hz}}$ have been the “work-horses” of PTB’s biomagnetism research and development since the 1990ies [4]. Shown is a medium-sized ($3.3\text{ mm} \times 3.3\text{ mm}$) general purpose cart-wheel-type SQUID magnetometer

Right: The recently developed “SQUID current sensor” [5] which forms the basis for the SQUID system with a ten times lower noise floor [3].

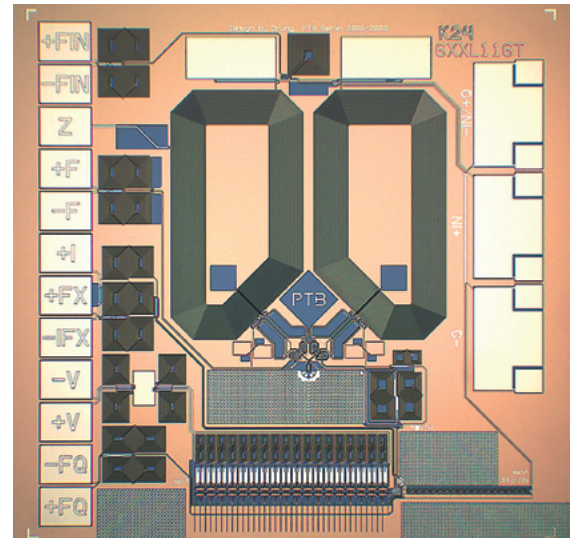
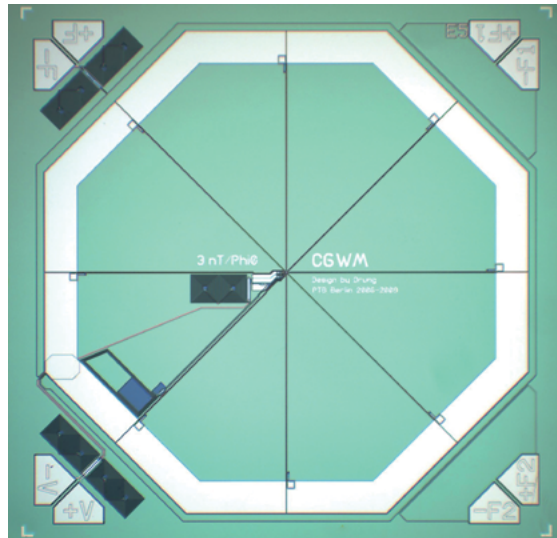
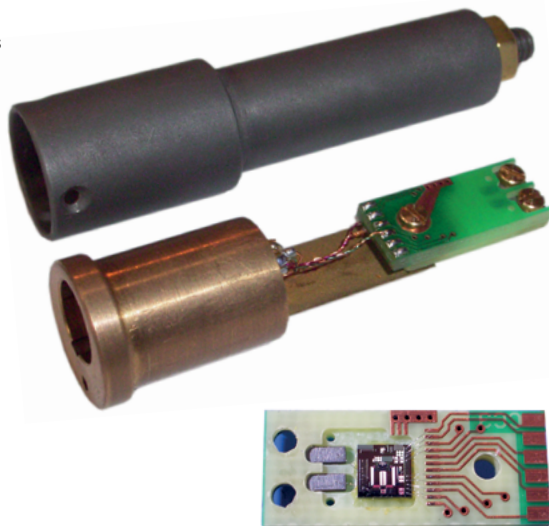


Figure 6.2:

Commercial SQUID current sensors package. The superconducting connection to the SQUID input coil is realized via screw contacts. Commercial SQUID-based noise thermometer MFFT-1 for sub-Kelvin thermometry (right). For low-noise operation, the SQUID sensors are enclosed in a superconducting Nb shield. (Courtesy of Magnicon GmbH, Hamburg und Berlin)



are used, which must be kept “only” at temperatures of liquid nitrogen. But the noise level of HTc-SQUIDs is more than an order of magnitude higher compared to LTc-SQUIDs [6]. In addition, manufacturing and operation of HTc-sensors suffers from a number of technical problems. It is difficult to make pickup coils out of the ceramic material of HTc-SQUIDs. This excludes the design of vertical HTc-gradiometer coils, i.e. a 3-dimensional coil system of two or more inversely wound pickup loops. For LTc-SQUIDs, gradiometer-based common mode rejection saves a lot of effort in magnetic shielding that is otherwise needed to suppress external perturbations. Therefore, gradiometer systems based on LTc-SQUIDs are the established sensors for virtually all of the several hundred commercial multichannel magnetoencephalography (MEG) devices that are operated worldwide for brain research and neurological diagnostics.

OPMs

OPMs (Optically Pumped Magnetometers) have an even longer history than SQUIDs. In the late 1950s the response of atomic spins to an external magnetic field was suggested as an efficient magnetometer [7]. OPMs make use of a vapor of atoms which carry an unpaired electron spin (typically alkali atoms) and can absorb circular polarized light up to saturation. In the presence of a magnetic field, the spins precess about the magnetic field axis with an angular velocity that is proportional to the magnetic field. The deflection of the atomic spin in a magnetic field generates a change in the absorption that is taken as a measure of its strength.

OPMs were quickly implemented, mostly for military applications [8]. Compared to SQUIDs, their performance has been rather poor for many years, but the rise of optical pumping techniques [9] as well as the invention of the laser have pushed the field of atomic magnetometry to a new level. Today, the best atomic magnetometers have demonstrated sensitivities similar to those of the best SQUID magnetometers, even though their frequency band is much narrower [10].

OPMs are independent of costly resources such as liquid helium cryogenics. More importantly, OPMs can be miniaturized, so they offer key benefits due to their flexible handling. This led to the design of atomic magnetometers suitable for recording biomagnetic signals. In fact, chip scaled atomic magnetometers can be attached to the human thorax or skull just like electrodes (“magnetodes”) that are well established for conventional electrocardiography and electroencephalography. Pioneering studies have demonstrated the applicability of OPMs in magnetocardiography (MCG) [11], magnetoencephalography (MEG) [12], and the detection of nerve impulses [13]. In addition, OPMs have shown their potential for other

applications, such as magnetic resonance imaging [14] and magnetic source imaging [15].

Nowadays, OPMs are offered by commercial companies, just like SQUIDs. The bandwidth of these commercial systems is about one hundred Hertz, while their sensitivity is about an order of magnitude behind the sensitivity of SQUIDs. This is sufficient for many applications, in particular for most biomagnetic measurements.

A major drawback of OPMs is that, at present, common mode rejection by gradiometer operation of OPMs decreases their sensitivity significantly. Therefore, OPMs need a heavily shielded environment to display their full performance. PTB is in the fortunate position to make use of its “Berlin Magnetically Shielded Room 2” (BMSR-2), which, with its eight shielding layers, offers ideal conditions for any kind of measurements using OPMs. This is why in applications for MCG [16], MEG [17], and magnetorelaxometry [18], OPMs could show their full potential only in the BMSR-2 of PTB.

There are several medical applications where the flexibility of OPMs makes them superior to SQUIDs. One example is fetal magnetocardiography (fMCG). While the electric potential generated by the fetal heart at the abdomen of the mother is hardly measurable, its magnetic field is much stronger. But in practice there remains the problem of disentangling this signal from the much stronger signal of the mother’s heart. By putting OPM-magnetodes separately on the mother’s chest and abdomen, these two sources are much easier to separate [18]. For SQUIDs kept in liquid helium, such a setup would be difficult to realize, because the spatial separation of SQUIDs would require two separate Dewar vessels.

Also, for cardio- and neuromagnetic measurements of subjects or patients which are unable to suppress their motion, SQUIDs, being mounted rigidly in the helium bath of the Dewar vessel, are evidently not the adequate tool. This complicates or excludes biomagnetic investigations of babies, children, or patients suffering from motional disorders (e.g. Parkinson’s disease), or studies which require unconstrained movements of the subject (e.g. MEG of spatial navigation or MCG under exercise). This is no problem for OPM-magnetodes which can easily be fixed at the head or thorax and can thus be handled like EEG or ECG electrodes.

However, the motion of the subject with the OPMs fixed on the skin in an inhomogeneous magnetic field generates artifacts that may compromise the quality of the data. One elegant way to compensate for such artifacts is to reduce the magnetic inhomogeneity of the magnetic environment by a sophisticated magnetic shimming system, similar to what is well established for mag-

Zero-Field-OPM (QuSpin QZFM-gen-1)

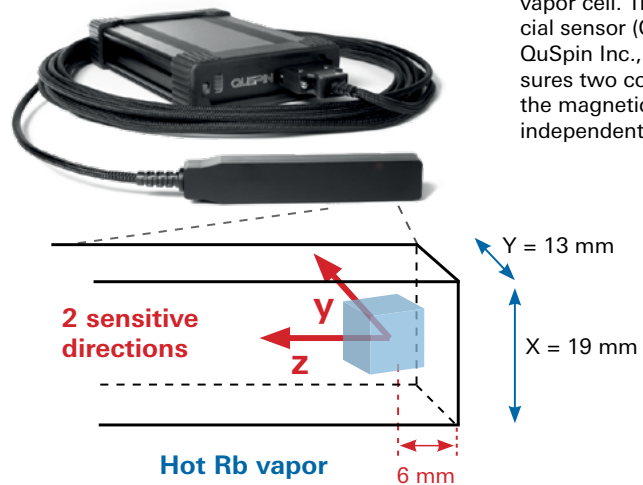


Figure 6.3: Unlike SQUIDs, OPM probes can be operated at room temperature. They do not rely on cooling, but rather slight heating of the vapor cell. This commercial sensor (QZFM-gen-1, QuSpin Inc., USA), measures two components of the magnetic field vector independently.

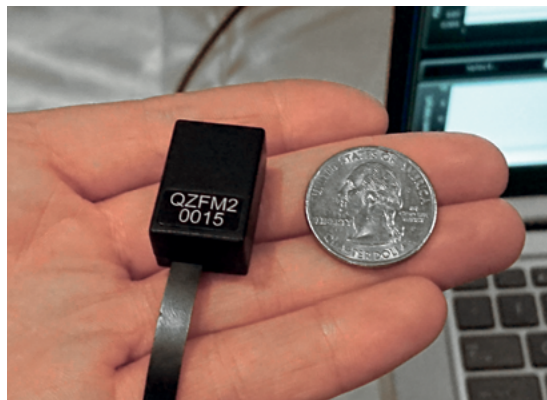


Figure 6.4: The latest generation of OPMs (QuSpin Inc., USA) is miniaturized down to the size of EEG-electrodes

netic resonance imaging devices [19]. Yet another (although costly) way to suppress such artifacts is to perform the measurement in a heavily shielded environment.

Magnetic shielding

While gradiometer based common mode rejection is the most popular (and least expensive) way to reduce external magnetic field perturbations in sensitive magnetic field measurements, the most forceful and rigorous way to deal with this interference is heavy magnetic shielding. Various types of magnetic shielding are currently in use:

- Static local compensation by electric coils driven by a constant current can be used to compensate the local earth magnetic field or other static magnetic fields.
- Local dynamic compensation of magnetic field changes by electric coils using a feedback loop. Field changes are measured by a reference magnetic field detector, such as a flux-gate magnetometer.



Figure 6.5:
Berlin Magnetically
Shielded Room 2
(BMSR-2)

- Shielding by permalloy material (>75 % Ni) like mu-metal or Magnifier. In a room with walls of such high magnetic permeability (μ) material both static and dynamic fields are reduced.
- A radio-frequency shield made of a closed structure of conducting metal.
- An eddy current shield consisting of a closed layer of highly conductive material such as copper or aluminum.

For the Berlin magnetically shielded room 2 (BMSR-2), all these techniques are applied. Assembly of BMSR-2 started in 1999 and regular operation began in 2004. This relatively long time span is due to the high research and development activity that PTB had to invest, in order to optimize the performance of BMSR-2, in particular in the field of degaussing technology. The walls of BMSR-2 consist of seven layers of mu-metal, one of aluminum within an rf shield. Further active shielding at very low frequencies is facilitated by compensation coils driven by feedback control. This improves the shielding factor by another 2 orders of magnitude at 0.01 Hz. With a shielding factor of 10^7 at 0.01 Hz and a residual static field below one nanotesla in its central volume of 1 m^3 , it is the strongest MSR in the world that is presently operational. Recently, BMSR-2 was upgraded with an additional inside shield that further improves its shielding performance in terms of temporal stability and homogeneity of the residual field by a factor of 10.

BMSR-2 is a walkable large size room with a special sliding door for quick access. It provides an inside volume of $2.9 \times 2.9 \times 2.8 \text{ m}^3$. Vibrations in BMSR-2 are $< 5 \mu\text{m}$ due to a stiff construction and passive damping by a massive and heavy concrete foundation. When the four sliding doors of the room are closed, a pneumatic mechanism generates

a tight connection between the shielding layers of the doors and the shielding layers of the walls. The sliding door concept is the cause of another feature of BMSR-2 that is most important for the practical work: After opening and closing, the field in the center returns close to its previous value after 30 s without the need of a new degaussing.

In addition to a high shielding performance, sensitive magnetic measurements require the reduction of residual fields that are generated by the magnetization of the walls and equipment inside the room. This includes the choice of material for the experimental setup and, in particular, the technique of degaussing the mu-metal walls of magnetically shielded rooms [20][21]. Degaussing is achieved by an alternating current in a coil around the shielding material which decreases the magnetization slowly from cycle to cycle from saturation towards zero. In this context PTB coined the expression “equilibration” for the degaussing procedure in the presence of an outside or inside magnetic field.

Recently, BMSR-2 was upgraded to “BMSR-2.1” which now has the following improved performance:

- The temperature of the BMSR-2.1 is stabilised from $\Delta T \leq 1\text{K}$ to $\Delta T \leq 100 \text{ mK}$ by a newly installed air-conditioning system.
- The BMSR-2.1 can be degaussed by an automated procedure in less than 5 minutes to reach a residual field below 1 nT
- The ac shielding factor is $\geq 300\text{k}$ at 10 mHz due to a newly installed innermost μ metal layer.
- The field homogeneity around the center of the BMSR-2 chamber is $\leq 2.2 \text{ pT/cm}$ at 2.6 μT due to the newly installed in-wall square Helmholtz coils.

Fundamental research

In addition to the outstanding magnetically shielded environment and the availability of ultra-sensitive magnetic sensors, PTB has developed and established the technology of generating hyperpolarized nuclei of noble gases like ^3He or ^{129}Xe by optical pumping. This offers the unique chance to combine these technologies by measuring the nuclear precession of noble gases in a weak field inside BMSR-2 using a SQUID or OPM detector. Since the coherence lifetime of the nuclear net magnetization in homogeneous fields of a few microtesla can reach up to 100 h, this enables measurements of the Larmor precession frequency with an uncertainty in the nanohertz range [22].

This outstanding resolution opens a new access for studying fundamental physics. Precision measurements of nuclear spin precession frequency with this extreme resolution may reveal the presence of minute interactions of the spin system with their environment which go beyond the physics of the standard model, such as e.g. symmetry violations, interaction with dark matter, or violation of the Lorentz invariance. In collaboration with various scientists specialized in these fields, PTB has addressed some of these open problems of fundamental physics. By high resolution spin precession measurements, it was possible to lower the upper limit for the interaction

- of nuclear spins with a hypothetical cosmic background field that may violate Lorentz invariance [23] [24],
- with an externally applied electric field due to the presence of a nuclear electric moment that violates CP symmetry [25].
- of bound neutrons with unpolarized nucleons mediated by axions – a potential constituent of dark matter [26]

In addition, a method was suggested to measure the potential interaction of nuclei with dark matter by the identification of minute side bands in the resonance line [27] [28].

In the future, these fundamental studies will benefit from the upgraded performance of BMSR-2.1 and the continuously improving SQUID and OPM sensor technology.

Literatur

- [1] US patent US3363200 A (1964)
- [2] Drung D, Aßmann C, Beyer J, Kirste A, Peters M, Ruede F, Schurig T (2007) IEEE Trans Appl Supercond 17,2
- [3] Storm JH, Hömmen P, Drung D, Körber R (2017) An ultra-sensitive and wideband magnetometer based on a superconducting quantum interference device. Appl Phys Lett 110:072603
- [4] Drung, D. and Koch, H. (1994). An integrated dc SQUID magnetometer with variable additional positive feedback, Supercond. Sci. Technol. 7, pp. 242–245.
- [5] Drung, D. and Beyer, J. (2017) Application in Superconducting Quantum Interference Devices SQUIDs, in: Josephson Junctions: History, Devices, and Applications, Pan Stanford Publishing
- [6] Drung D, Ludwig F Müller, W, Steinhoff U, Trahms L, Koch H, Shen YQ, Jensen MB, Vase P, Holst T, Freltoft T, Curio G (1996) Integrated YBaCuO magnetometer for biomagnetic measurements. Appl Phys Lett 68:1421-1423.
- [7] H. G. Dehmelt, (1958) Spin Resonance of Free Electrons Polarized by Exchange Collisions, Phys Rev 109:381
- [8] A.R. Keyser, J.A. Rice, L. D. Scheerer, (1961) A metastable helium magnetometer for observing small geomagnetic fluctuations, J Geophys Res, 66(12):4163
- [9] Happer W (1972) Optical Pumping, Rev Mod Phys 44:169
- [10] Dang HB, Maloof, AC, Romalis, M. V. (2010) Ultrahigh sensitivity magnetic field and magnetization measurements with an atomic magnetometer Appl Phys Lett 97(15):151110
- [11] Bison G, Castagna N, Hofer A, Knowles P, Schenker JL, Kasprzak M, Saudan H, Weis A (2009) A room temperature 19-channel magnetic field mapping device for cardiac signals. Appl Phys Lett 95:173701
- [12] Xia H, Ben-Amar Baranga A, Hoffman D, Romalis MV (2006) Magnetoencephalography with an atomic magnetometer, Appl Phys Lett 89:211104
- [13] Jensen K, Budvytyte R, Thomas RA, Wang T, Fuchs AM, Balabas MV, Vasilakis G, Mosgaard LD, Stærkind HC, Müller JH, Heimburg T, Olesen S-P, Polzik ES (2016) Non-invasive detection of animal nerve impulses with an atomic magnetometer operating near quantum limited sensitivity. Scientific Reports 6:29638
- [14] Xu S, Yashchuk VV, Donaldson MH, Rochester SM, Budker D, Pines A (2006) "Magnetic resonance imaging with an optical atomic magnetometer. Proc Natl Acad Sci 103:12668-12671
- [15] Dolgovskiy V, Fescenko I, Sekiguchi N, Colombo S, Lebedev V, Zhang J, Weis A (2016) A magnetic source imaging camera. Appl Phys Lett 109:023505
- [16] Knappe S, Sander TH, Wiekhorst F, Kitching J, Trahms L (2010) Cross-validation of microfabricated atomic magnetometers with SQUIDs for biomagnetic applications, Appl Phys Lett, 97:133703.
- [17] Sander TH, Preusser J, Mhaskar R, Kitching J, Trahms L, Knappe S (2012) Magnetoencephalography with a chip scale atomic magnetometer, Biomed Opt Express 3(5):981–990.
- [18] Alem O, Sander TH, Mhaskar R, LeBlanc J, Eswaran H, Steinhoff U, Okada Y, Kitching J, Trahms, Knappe S (2015) Fetal magnetocardiography measurements with an array of microfabricated optically pumped magnetometers, Phys Med Biol 60:4797–4811
- [19] Boto E, Holmes N, Leggett, J, Roberts G, Shah V, Meyer SS, Munoz LD, Mullinger KJ, Tierney TM, Bestmann S, Barnes GR, Bowtell R, Brookes, MJ (2018) Moving magnetoencephalography towards real-world applications with a wearable system, Nature 555:657–661
- [20] Thiel F, Schnabel A, Knappe-Grüneberg S, Stollfuß D, Burghoff M (2013) Proposal of a Demagnetization Function IEEE Transact Magn, 43(6)

- [21] Voigt J, Knappe-Grüneberg S, Schnabel A, Körber R, Burghoff M (2013) Measures to reduce the residual field and field gradient inside a magnetically shielded room by a factor of more than 10, *Metrol Meas Syst*, 21, 2, 239–248
- [22] Gemmel C, Heil W, Lenz D, Ludwig C, Thulley K, Sobolev Y, Burghoff M, Knappe-Grüneberg, S, Kilian W, Müller W, Schnabel A, Seifert F, Trahms, L Baeßler S (2010) Ultra-sensitive magnetometry based on free-precession of nuclear spins, *Eur Phys J D*, 57:303-320.
- [23] Gemmel C, Heil W, Karpuk WS, Lenz K, Sobolev Yu, Tullney K, Burghoff M, Kilian W, Knappe-Grüneberg S, Müller W, Schnabel A, Seifert F, Trahms L, Schmidt U (2010) Limit on Lorentz and CPT violation of the bound neutron using a free precession $^3\text{He}/^{129}\text{Xe}$ comagnetometer., *Phys Rev D*, 82:111901.
- [24] Allmendinger F, Burghoff M, Heil W, Karpuk S, Kilian W, Knappe-Grüneberg S, Müller W, Schmidt U, Schnabel A, Seifert F, Sobolev Y, Trahms L, Tullney K (2013) Searches for Lorentz violation in $^3\text{He}/^{129}\text{Xe}$ clock comparison experiments, *Hyperfine Interact* 215:15–23.
- [25] Sachdeva N, Fan I, Babcock E, Burghoff M, Chupp TE, Degenkolb S, Fierlinger P, Haude S, Kraegeloh, Kilian W, Knappe-Grüneberg S, Kuchler F, Liu T, Marino M, Meinel J, Rolfs K, Salhi Z, Schnabel A, Singh JT, Stuiber S, Terrano WA, Trahms L, Voigt J (2019) New Limit on the Permanent Electric Dipole Moment of ^{129}Xe Using ^3He Comagnetometry and SQUID Detection, *Phys Rev. Lett* 123, 143003
- [26] Tullney K, Allmendinger F, Burghoff M, Heil W, Karpuk S, Kilian W, Knappe-Grüneberg, S, Müller W, Schmidt U, Schnabel A, Seifert F, Sobolev Y, Trahms L (2013) Constraints on spin-dependent short-range interaction between nucleons, *Phys Rev Lett*, 111:100801.
- [27] Graham PW, Kaplan DE, Mardon J, Rajendran S, Terrano WA, Trahms L, Wilkason T(2018) Spin precession experiments for light axionic dark matter *Phys Rev.D* 97,055006
- [28] Garcon A, Aybas D, Blanchard JW, Centers G, Figueroa NL, Graham PW, Jackson Kimball DF, Rajendran S, Sendra MG, Sushkov AO, Trahms L, Wang T, Wickenbrock A, Wu T, Budker D (2018) The Cosmic Axion SpinPrecession Experiment (CASPEr): a dark-matter search with nuclear magnetic resonance *Quant Sci Technol* 3:014008.